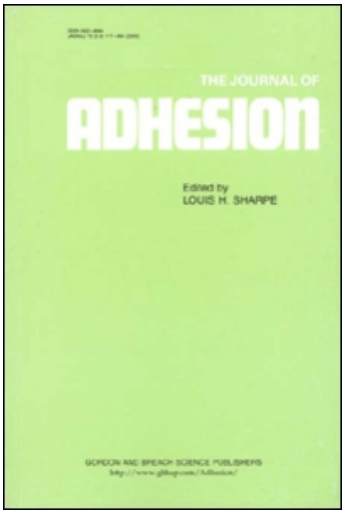

The Journal of Adhesion

Publication details, including instructions for authors and subscription information:
http://www.informaworld.com/smpp/title~content=t713453635

Pullout of a Rigid Insert Adhesively Bonded to an Elastic Half Plane

G. K. Haritos[a]; L. M. Keer[b]
[a] Department of Aeronautics and Astronautics, Air Force Institute of Technology, Wright Patterson Air Force Base, OH, U.S.A. [b] Department of Civil Engineering, Northwestern University, Evanston, II, U.S.A.

To cite this Article Haritos, G. K. and Keer, L. M.(1985) 'Pullout of a Rigid Insert Adhesively Bonded to an Elastic Half Plane', The Journal of Adhesion, 18: 2, 131 — 150
To link to this Article: DOI: 10.1080/00218468508079675
URL: http://dx.doi.org/10.1080/00218468508079675

J. Adhesion, 1985, Vol. 18, pp. 131–150
0021–8464/85/1802–0131 $18.50/0

Printed in the United Kingdom

Pullout of a Rigid Insert Adhesively Bonded to an Elastic Half Plane

G. K. HARITOS

Department of Aeronautics and Astronautics, Air Force Institute of Technology, Wright Patterson Air Force Base, OH 45433, U.S.A.

and

L. M. KEER

Department of Civil Engineering, Northwestern University, Evanston, Il 60201, U.S.A.

(*Received January 20, 1984; in final form September 7, 1984*)

The problem considered here is that of a finite, rigid insert partially embedded in and adhesively bonded to an elastic half plane. Two distinct problems are investigated: the shear pullout of the insert without rotation, which takes into account the adhesive's resistance to shear deformation, and an opening problem which incorporates the adhesive's resistance to normal deformation. This latter problem assumes the presence of an edge crack in the half plane subjected to opening pressure which equals in magnitude the normal stress distribution due to the pullout problem. These mixed boundary value problems are governed by singular integral or integrodifferential equations. Numerical results are obtained *via* a technique introduced by Gerasoulis and Srivastav. Several important physical quantities are calculated, such as the shear and normal stress distributions along the bonded interface, and the crack opening displacements.

1. INTRODUCTION

The problem of a rigid insert partially embedded in and adhesively bonded to an elastic half space is considered within the context of plane elastostatics. The thickness of the insert is assumed to be negligible. It is also assumed that the adhesive's deformation remains in the linear elastic range. The thickness of the adhesive is small, but not

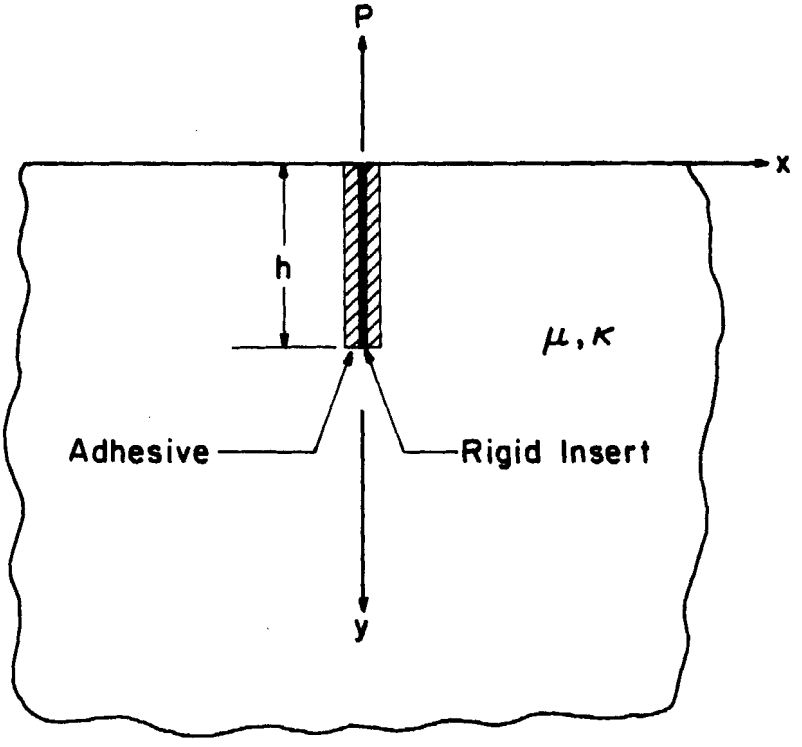

FIGURE 1 Geometry and coordinate system for a partially embedded finite rigid insert undergoing shear displacement.

negligible. The adhesive layer is modeled as a series of linear springs subjected to shear or tension.

Loading is applied to this insert so that it translates in the vertical direction without rotation (Fig. 1). Of interest here are the shear and normal stresses generated along the bonded interface. These stresses will cause the adhesive to undergo both shear and normal deformation. Two distinct problems are considered: the shear pullout problem already described, which takes into account the adhesive's resistance to shear deformation, and the opening problem, described next, which considers the adhesive's resistance to normal deformation. The opening problem assumes an edge crack in a half space subjected to opening pressure which is equal in magnitude to the normal stress distribution resulting from the pullout problem. In this case, the adhesive

material's resistance to normal deformation is used to reduce the opening pressure's intensity. The physical quantities of interest in this problem are the crack opening displacements.

The problems considered here can be viewed as appropriate idealizations for studying two separate, yet similar, classes of problems. In the context in which they have been presented thus far, they are problems in plane strain. As such, they are appropriate for investigating the mechanics of interface failure in fiber-reinforced composite materials. The more realistic case of adhesive failure (adhesive material allowed to deform non-linearly) is currently being considered by the authors. As pointed out by Brussat and Westmann[1] and by Chamis,[2] interface damage is believed to be one of the earliest forms of damage in such composite materials. The subject of fiber debonding has attracted several investigators over the last several years (see references 1 and 2 for summary). One fundamental question that seems to remain still unanswered, and which is addressed in this paper, is whether the surfaces of a crack at the fiber-matrix interface are traction-free, or remain in contact. It is suggested by Westmann that the debonded surfaces may be open or closed depending on the relative magnitude of the applied *versus* the residual stresses.[1]

In the generalized plane stress context, these problems deal with finite rigid inserts of negligible width, partially embedded within a semi-infinite elastic sheet. In this case, the results obtained may serve to understand better the stress distribution at the bonded interface of dissimilar materials, where one is significantly more rigid than the other. More importantly, an extension of this work which will be addressed in the near future will consider the case of an elastic insert of finite width embedded in an elastic half plane. That problem would be applicable to several physical situations, such as the primary adhesively bonded aircraft fuselage being considered by the U.S. Air Force.[3]

The problems are formulated as mixed boundary value problems. This leads to singular integral or integrodifferential equations, which are solved numerically for the desired physical quantities by use of a numerical technique introduced by Gerasoulis and Srivastav.[4,5] The material constants selected for the adhesive and for the adherend material correspond to materials commercially available.

2. FORMULATION AND BASIC EQUATIONS

The formulation of the problems considered in this investigation makes use of certain results obtained in two earlier papers.[6,7] Those papers considered the problem of a finite, rigid block embedded in an elastic half space,[6] and that of a rectangular trench in an elastic half plane.[7] The problems were formulated by superposition of the solutions for rigid line inclusions and cracks, respectively, parallel and perpendicular to the free surface of the half plane. The results which pertain to the present work are those derived in reference 6 for a rigid line inclusion perpendicular to the free surface of the half plane, and the ones derived in reference 7 for an edge crack.

A. Rigid insert pullout: The shear mode

A rigid line inclusion is partially embedded in and bonded to an elastic half plane, $y>0$, so that it occupies the line segment $0 \leqq y \leqq h$, $x=0$ in the half plane. The inclusion is loaded by a force P acting along the negative y-axis as shown in Fig. 1. The material properties of the half plane are taken as μ and κ; μ is the shear modulus, while κ is related to Poisson's ratio v by $\kappa = 3\text{-}4v$ (plane strain), or $\kappa = (3\text{-}v)/(1+v)$ (generalized plane stress). The inclusion is assumed to be bonded to the half plane by use of some adhesive material in such a manner that there are no discontinuities in the application of the adhesive to the inserted inclusion, and no significant variations in its thickness, which is also assumed to be negligibly small (less than 5×10^{-3} in.). The adhesive is assumed to behave as a number of linear springs, subjected to shear in this case. The stiffness of these springs, k_s, is computed using the mechanical properties of the adhesive. This is discussed in detail in a later section.

The shear stress developed in the adhesive (and transferred to the half plane) may be written as follows:

$$\tau_{xy}(x,y) = k_s\,[u_y(x,y) - u_o];\; x=0,\; 0 \leqq y \leqq h \tag{2.1}$$

Here, u_o is a constant representing the y-displacement of the rigid inclusion, while u_y designates the y-displacement of the half plane material. Thus, the quantity in the brackets gives the displacement of the insert relative to the half plane, which is also the shear deformation of the adhesive. The constant k_s is, as defined earlier, the stiffness of the adhesive modeled as a shear spring.

The displacement u_o cannot be calculated. Differentiation of (2.1) with respect to y yields the following equation:

$$\frac{\partial}{\partial y}[u_y(x,y)] = \frac{1}{k_s}\frac{\partial}{\partial y}[\tau_{xy}(x,y)];\ x = 0,\ 0 \leqq y \leqq h \tag{2.2}$$

The left-hand side of eqn (2.2) is given in terms of a singular integral equation derived in reference 6 using integral transform techniques.[8,9] When that result is used, equation (2.2) takes on the following form:

$$\frac{1}{4\pi(\kappa+1)\mu}\left\{2\kappa\int_o^h \frac{D(t)dt}{y-t} + \int_o^h D(t)\left[\frac{(\kappa-1)^2}{y+t} - \frac{2[2t-\kappa(y+t)]}{(y+t)^2}\right.\right.$$

$$\left.\left. + \frac{8yt}{(y+t)^3}\right]dt\right\} = \frac{1}{k_s}\frac{\partial}{\partial y}[\tau_{xy}(x,y)];\ x = 0,\ 0 \leqq y \leqq h \tag{2.3}$$

The function $D(y)$ is the unknown shear stress discontinuity associated with the rigid inclusion and it is defined as follows:

$$D(y) = \tau_{xy}^{(2)} - \tau_{xy}^{(1)};\ x = 0,\ 0 \leqq y \leqq h \tag{2.4}$$

The superscripts (1) and (2) denote the regions to the left and to the right of the inclusion, respectively. The symmetry of the problem requires that $\tau_{xy}^{(2)} = -\tau_{xy}^{(1)}$. Clearly then, the following relation must hold between τ_{xy} and D:

$$\tau_{xy}(0,y) = \frac{1}{2}D(y);\ 0 \leqq y \leqq h \tag{2.5}$$

Substitution of eqn (2.5) into eqn (2.3) leads to the following integrodifferential equation in the unknown $D(y)$:

$$\int_o^h \frac{D(t)dt}{t-y} + \int_o^h D(t)K(y,t)dt = -\frac{\pi(\kappa+1)\mu}{\kappa k_s}\frac{\partial}{\partial y}[D(y)];\ x = 0,\ 0 \leqq y \leqq h \tag{2.6}$$

Here, the function $K(y,t)$ is given as follows:

$$K(y,t) = -\frac{1}{2\kappa}\left[\frac{(\kappa-1)^2}{y+t} - \frac{2[2t-\kappa(y+t)]}{(y+t)^2} + \frac{8yt}{(y+t)^3}\right] \tag{2.7}$$

It should be noted here that the expression for $\frac{\partial}{\partial y}u_y$ substituted in

eqn (2.2) to obtain eqn (2.3) was derived in reference 6 so that the following conditions are satisfied:

$$\left.\begin{aligned} u_x^{(2)} - u_x^{(1)} &= 0 \\ u_y^{(2)} - u_y^{(1)} &= 0 \end{aligned}\right\} x = 0,\ 0 \leqq y \leqq h; \tag{2.8}$$

$$\tau_{yy} = \tau_{xy} = 0;\ y = 0,\ 0 \leqq |x| < \infty \tag{2.9}$$

Equation (2.8) requires that the displacements on either side of the inclusion be continuous, while eqn (2.9) clears the half plane surface of stresses.

Equilibrium in the y-direction is satisfied by requiring that the following relationship hold:

$$\int_0^h D(y)dy = P \tag{2.10}$$

Thus, the solution of the shear pullout of the rigid insert problem consists of solving the governing integrodifferential equation (2.6) for the unknown $D(y)$ subject to the equilibrium condition (2.10). The solution is obtained by means of numerical methods as will be discussed in the numerical analysis section.

Once $D(y)$ has been determined the stresses generated along the bond line are readily obtained. The shear stresses are computed using eqn (2.5), while the normal stresses are obtained from the following:[6]

$$\tau_{xx}(0,y) = \frac{\kappa - 1}{2\pi(\kappa + 1)} \left\{ \int_0^h \frac{D(t)dt}{t - y} + \int_0^h D(t)\ L(y,t)\ dt \right\};\ 0 \leqq y \leqq h \tag{2.11}$$

The function $L(y, t)$ is defined as:

$$L(y,t) = \frac{1}{\kappa - 1} \left[\frac{3\kappa - 1}{y + t} + \frac{2(3t - \kappa y)}{(y + t)^2} - \frac{8yt}{(y + t)^3} \right] \tag{2.12}$$

B. Rigid insert pullout: The opening mode

The normal stress distribution generated along the bond line of the insert during pullout is now applied as opening pressure on an edge crack in the half plane. It is assumed that the crack extends from $y = 0$ to $y = h$ and it is located at the bond line, $x = 0$. The adhesive

material in this case behaves as a number of linear springs of stiffness k subjected to tension. Thus, it resists the opening of the crack by providing a stress equal to $k(COD/2)$ which reduces the intensity of the applied opening pressure. The crack opening displacement (COD) is the distance between the crack surfaces.

The normal stresses within a half plane containing an edge crack are given in reference 7. The bond line stresses are given in terms of the dislocation density $B(y)$ as:

$$\tau_{xx}^{c}(0, y) = \frac{2\mu}{\pi(\kappa+1)}\left\{\int_0^h \frac{B(t)dt}{t-y} + \int_0^h B(t)\left[\frac{1}{y+t} + \frac{2t(y-t)}{(y+t)^3}\right]dt\right\}; \quad 0 \leqq y \leqq h \quad (2.13)$$

Here, μ and κ are the half space material constants given earlier. The superscript c is used to distinguish these normal stresses from the ones associated with the shear pullout problem. The dislocation density $B(y)$ is defined as:

$$B(y) = \frac{\partial}{\partial y}[u_x^{(2)} - u_x^{(1)}]; \; x = 0, \; 0 \leqq y \leqq h \quad (2.14)$$

The superscripts (1) and (2) refer to the half plane regions to the left and to the right of the crack, respectively. The singular integral equation (2.13) was derived in reference 7 using integral transform techniques.

The governing equation for this problem is formulated by replacing τ_{xx}^{c} in eqn (2.13) by the difference between the opening pressure and the spring-induced resisting stress. This leads to the following equation:

$$\int_0^h \frac{B(t)dt}{t-y} + \int_0^h B(t)\left[\frac{1}{y+t} + \frac{2t(y-t)}{(y+t)^3}\right]dt = \frac{\pi(\kappa+1)}{2\mu}\left[-\tau_{xx}(0,y) + k\left(\frac{COD}{2}\right)\right]; \; x = 0, \; 0 \leqq y \leqq h \quad (2.15)$$

As stated earlier, the opening pressure τ_{xx} is the one obtained from the shear pullout case, and k is the equivalent spring constant for the adhesive. Following eqn (2.14) the crack opening displacement at y is given by:

$$COD(y) = [u_x^{(2)} - u_x^{(1)}]_y = -\int_y^h B(t)dt;\ 0 \leqq y \leqq h,\ x = 0 \quad (2.16)$$

Equations (2.15) and (2.16) are solved numerically for the crack opening displacements and the dislocation densities. The procedure is discussed in detail in the next section.

3. NUMERICAL ANALYSIS

The procedure for obtaining numerical results for the shear pullout of the rigid insert problem is discussed first. The governing integrodifferential equaltion, (2.6), and the equation of equilibrium, (2.10), are normalized by introducing the following variable changes:

$$y = \tfrac{1}{2}h(\bar{y} + 1);\ t = \tfrac{1}{2}h(\bar{t} + 1) \quad (3.1)$$

The function $D(t)$ is non-dimensionalized and given square root singularities at its ends by making the following substitution:

$$D(t) = \frac{2P}{h}\bar{D}(\bar{t})(1 - \bar{t}^2)^{-0.5} \quad (3.2)$$

It should be noted that the square root singularities are assumed here merely for computational convenience, and they are only used in the first iteration.* This is discussed further in the next section.

With these changes, equations (2.6) and (2.10) take on the following forms:

$$\int_{-1}^{1} \frac{\bar{D}(\bar{t})(1 - \bar{t}^2)^{-0.5}dt}{\bar{t} - \bar{y}} + \int_{-1}^{1} \bar{D}(\bar{t})(1 - \bar{t}^2)^{-0.5}\bar{K}(\bar{y}, \bar{t})d\bar{t}$$

$$= \frac{2\pi(\kappa + 1)\mu}{\kappa k_s h}\frac{\partial}{\partial \bar{y}}[\bar{D}(\bar{y})(1 - \bar{y}^2)^{-0.5}];\ x = 0,\ -1 \leqq \bar{y}, \bar{t} \leqq 1; \quad (3.3)$$

$$\int_{-1}^{1} \bar{D}(\bar{t})(1 - \bar{t}^2)^{-0.5}d\bar{t} = 1;\ x = 0,\ -1 \leqq \bar{t} \leqq 1 \quad (3.4)$$

The function $\bar{K}(\bar{y}, \bar{t})$ is given next:

$$\bar{K}(\bar{y}, \bar{t}) = \frac{1}{2\kappa}\left[-\frac{(\kappa - 1)^2}{\bar{y} + \bar{t} + 2} + \frac{2[2(\bar{t} + 1) - \kappa(\bar{y} + \bar{t} + 2)]}{(\bar{y} + \bar{t} + 2)^2} - \frac{8(\bar{y} + 1)(\bar{t} + 1)}{(\bar{y} + \bar{t} + 2)^3}\right] \quad (3.5)$$

* A discussion of the order of singularities for the case where the adhesive is taken as rigid is given by Hein and Erdogan.[10]

The spring constant k_s is estimated from the mechanical properties of adhesive materials representative of the ones used in industry.[3] A simple dimensional analysis carried out on eqn (2.1) shows that the appropriate units for the equivalent spring constant are [force/(length)^3]. If G is the shear modulus of the adhesive and t is its average thickness when applied to such materials as aluminium or titanium alloys, then k_s is given by:

$$k_s = \frac{G}{t} \tag{3.6}$$

Numerical results were obtained for several values of k_s. The range of values considered was based on two adhesives which are used in industry. Their properties will be discussed in the next section.

The kernel of the right-hand side of eqn (3.3) has a Cauchy-type singularity. The numerical method introduced by Gerasoulis and Srivastav[4,5] is used here to reduce the right-hand side of (3.3) to a system of linear algebraic equations. The method consists of replacing the integral equation by integral relations at a set of points. Piecewise linear functions are then used to approximate the integrand at a finite set of (collocation) points. The values of the unknown function at those points are then obtained *via* closed form integration.

Equation (3.3) is thus reduced to a system of linear algebraic equations which may be written in matrix form as follows:

$$\frac{1}{c_1}[A]\{\bar{D}(\bar{t})\} = -\left\{\frac{\partial}{\partial \bar{y}}[\bar{D}(\bar{y})(1-\bar{y}^2)^{-0.5}]\right\} \tag{3.7}$$

Here, the symbol [ ] denotes a two-dimensional matrix, while { } denotes a column matrix. The integration points $\bar{t}_k$, $k = 1, 2, \ldots, 2N+1$, are chosen to be equally spaced in the interval $-1 \leqq \bar{t}_k \leqq 1$, and the collocation points $\bar{y}_j$ are chosen in the same interval such that $\bar{t}_j \leqq \bar{y}_j \leqq \bar{t}_{j+1}$, $j = 1, 2, \ldots, 2N$. The matrix A contains the coefficients of the unknowns $\bar{D}(\bar{t}_k)$ and they are as given in reference 5. The constant c_1 is given by

$$c_1 = \frac{2\pi(\kappa+1)\mu}{\kappa k_s h} \tag{3.8}$$

The solution is obtained using an iterative method. As a first

approximation, $\bar{D}(\bar{t}_k)$ are set equal to the results obtained from the solution of the problem which assumes that the insert is *perfectly* bonded at the half plane, *i.e.*, the case where the spring stiffness k_s tends to infinity. Simple matrix multiplication leads to numerical values for the slopes of the normalized stress discontinuities at the collocation points $\bar{y}_j$. These results are fitted using cubic splines, and then numerically integrated using Gauss' formula (see, *e.g.*, references 11 and 12) to obtain values for $\bar{D}$ at $\bar{t}_k$. These values are normalized so that the equilibrium equation (3.4) is satisfied, and the results are substituted back into eqn (3.7) for the next iteration. This process is repeated until a convergence criterion is satisfied. Upon convergence, the results are used to compute the stresses generated in the contact region. The shear stresses are obtained from eqn (3.2). To compute the normal stresses, equation (2.11) is first normalized using eqns (3.1) and (3.2); this yields the following expression:

$$\tau_{xx}(\bar{y}) = \frac{P}{h}\frac{(\kappa-1)}{\pi(\kappa+1)}\left\{\int_{-1}^{1}\frac{\bar{D}(\bar{t})(1-\bar{t}^2)^{-0.5}d\bar{t}}{\bar{t}-\bar{y}} + \int_{-1}^{1}\bar{D}(\bar{t})(1-\bar{t}^2)^{-0.5}[(\bar{y},\bar{t})d\bar{t}\right\};\ x=0,\ -1\leqq\bar{y}\leqq 1 \quad (3.9)$$

The function $\bar{L}(\bar{y},\bar{t})$ is given by

$$\bar{L}(\bar{y},\bar{t}) = \frac{1}{\kappa-1}\left[\frac{3\kappa-1}{\bar{y}+\bar{t}+2} + \frac{2[3(\bar{t}+1)-\kappa(\bar{y}+1)]}{(\bar{y}+\bar{t}+2)^2} - \frac{8(\bar{y}+1)(\bar{t}+1)}{(\bar{y}+\bar{t}+2)^3}\right] \quad (3.10)$$

Equation (3.9) may now be written as a system of linear algebraic equations exactly as it was done with the left hand side of eqn (3.3). Numerical values for the normal stresses at collocation points are obtained by multiplying the matrix of the coefficients of this system of equations by the solution vector $\{\bar{D}(\bar{t})\}$.

The Gerasoulis–Srivastav technique[4] is also used to obtain numerical results for the opening case. First, equation (2.15) is normalized and the dislocation densities are given singularities at the ends by making the following substitutions:

$$y = \tfrac{1}{2}h(\bar{y}+1);\ t = \tfrac{1}{2}h(\bar{t}+1);\ \text{(restated)} \quad (3.1)$$

$$B(t) = \frac{P}{\mu h}\bar{B}(\bar{t})(1-\bar{t}^2)^{-0.5} \quad (3.11)$$

With these substitutions, equation (2.15) becomes:

$$\int_{-1}^{1} \frac{\bar{B}(\bar{t})(1-\bar{t}^2)^{-0.5}d\bar{t}}{\bar{t}-\bar{y}} + \int_{-1}^{1} \bar{B}(\bar{t})(1-\bar{t}^2)^{-0.5}$$

$$\left[\frac{1}{(\bar{y}+\bar{t}+2)} + \frac{2(\bar{t}+1)(\bar{y}-\bar{t})}{(\bar{y}+\bar{t}+2)^3}\right]d\bar{t} = \frac{\pi(\kappa+1)}{2}\frac{h}{P}\left[-\tau_{xx}(0,\bar{y})\right.$$

$$\left. + k(\frac{COD}{2})\right]; \; x = 0, \; -1 \leqq \bar{y} \leqq 1 \tag{3.12}$$

The equivalent spring constant for the adhesive in tension, k, is given by the following relation:

$$k = \frac{E}{t} \tag{3.13}$$

Numerical results were obtained for values of E corresponding to the range of G values used in the shear case. A detailed discussion of this is presented in the results and discussion section.

Equation (3.12) is reduced to a system of linear algebraic equations,[4] and then placed in matrix form as follows:

$$[M]\{\bar{B}(\bar{t})\} = c_2\frac{h}{P}\left\{-\tau_{xx}(0,\bar{y}) + k\left(\frac{COD}{2}\right)\right\} \tag{3.14}$$

The matrix $[M]$ contains the coefficients of the unknown normalized dislocation densities, and c_2 is given as

$$c_2 = \frac{\pi(\kappa+1)}{2} \tag{3.15}$$

Premultiplication of both sides of eqn (3.14) by the inverse of $[M]$ leads to the following relation:

$$\{\bar{B}(\bar{t})\} = c_2[M]^{-1}\frac{h}{P}\left\{-\tau_{xx}(0,\bar{y}) + k\left(\frac{COD}{2}\right)\right\} \tag{3.16}$$

The solution for this equation is also obtained *via* an iterative method. A first estimate of the values in the column matrix $\{-\tau_{xx}(0,\bar{y}) + k\left(\frac{COD}{2}\right)\}$ is made by setting them equal to some percentage of the opening pressures $\tau_{xx}(0,\bar{y})$. The matrix multiplication indicated at the right-hand side of eqn (3.16) leads to the initial estimate for

the dislocation densities $\bar{B}(\bar{t}_k)$. These values are next used to compute the corresponding crack opening displacements from eqn (2.16). First, equation (2.16) is normalized by making the substitutions given in (3.1) and (3.11). The resulting expression may be written in the following form:

$$\tfrac{1}{2}[COD]_\alpha = \tfrac{1}{2}[u_x^{(2)} - u_x^{(1)}]_\alpha = -\frac{P}{4\mu}\int_\alpha^1 \bar{B}(\bar{t})(1-\bar{t}^2)^{-0.5}d\bar{t}; \quad -1 \leqq \alpha \leqq 1 \tag{3.17}$$

The values of $\frac{1}{2}$ (COD) are needed at the collocation points $\bar{y}_j$. Values of $\bar{B}(\bar{t})$ have been calculated at the integration points $\bar{t}_k$; these values are numerically interpolated using cubic splines. Then, by setting $\alpha = \bar{y}_j$, Gaussian integration leads to the desired values of $\frac{1}{2}$ (COD) at $\bar{y}_j$. These results are then substituted into the right-hand side of (3.16) for the next iteration. This procedure is repeated until a convergence criterion is satisfied.

4. RESULTS AND DISCUSSION

The numerical analysis was carried out for $N = 9$ and $N = 17$, corresponding to 19 and 35 integration points, respectively. There was no significant difference between the two sets of results. The applied load P and the depth h were set equal to 1 for all cases. Results were obtaincd for a range of tensile and shear elastic moduli E and G. The values considered were set according to the properties of two commercially available adhesives. The first is a relatively rigid one, known as FM-73, manufactured by American Cyanamid, Bloomingdale Division. It is an elastomer-modified epoxy material. Its properties were experimentally determined by the Kearfott Division of Singer.[13] The second adhesive material is of relatively low rigidity; it is an experimental one component urethane adhesive produced by Goodyear coded AX37J922.[14] Average G, E, and t values for these materials are given in Table I.

The ratio E/G for the AX37J922 adhesive is equal to 2.907. Poisson's ratio for this material is approximately equal to 0.45. These values for E and G (Table I) are in good agreement with the theoretical relation between E, G, and v:

$$E = 2(1+v)G \tag{4.1}$$

However, the experimentally computed value of E for FM 73,[13] does

TABLE I
Experimentally determined properties of adhesives (references 13, 14)

	Shear tests		Tensile tests	
	Average Bond Line Thickness, t (inch)	Average Modulus, G (psi)	Average Bond Line Thickness, t (inch)	Average Modulus, G (psi)
FM 73	0.0047	84,000	0.0045	360,000
AX37J922	0.0050	15,000	0.0050	43,600

not correspond to the value given for G. When these values are substituted in eqn (4.1), the resulting value for ν is 1.14. Since ν cannot be greater than 0.5, the value used for E in this case was adjusted to be consistent with the one for the shear modulus. Taking $\nu = 0.35$ and $G = 84{,}000$ psi, equation (4.1) gives $E = 226{,}000$ psi; this value will be used in lieu of the one given in Table I. Values for k_s and k may now be computed following equations (3.6) and (3.13). Numerical results were obtained for eight sets of k_s, k values (see Table II). The ones coded B and G correspond to AX37J922 and FM 73, respectively. In addition, four intermediate sets of values were chosen at equal intervals between B and G (C-F), as well as two sets outside the B to G range (A, H).

TABLE II
Shear and tensile spring constants

Code	k_s(lbs/in^3)	k(lbs/in^3)
A	0.0022×10^7	0.042×10^7
B	0.3000×10^7	0.872×10^7
C	0.5878×10^7	1.702×10^7
D	0.8956×10^7	2.532×10^7
E	1.1934×10^7	3.362×10^7
F	1.4912×10^7	4.192×10^7
G	1.7890×10^7	5.022×10^7
H	2.0868×10^7	5.852×10^7

Two adherend materials were considered: The 7075–T6 aluminium alloy and the Ti-6A1-4V titanium alloy. Both of these materials find widespread application in aircraft structures. Material constants for the aluminium alloy are taken as $E = 10.4 \times 10^6$ psi, $\mu = 3.75 \times 10^6$ psi, and $\nu = 0.33$; the ones for the titanium are $E = 16 \times 10^6$ psi, $\mu = 6.4 \times 10^6$ psi, and $\nu = 0.34$. All results plotted here are the ones obtained for the plane strain case with $N = 17$, and with Ti-6A1-4V being the adherend material.

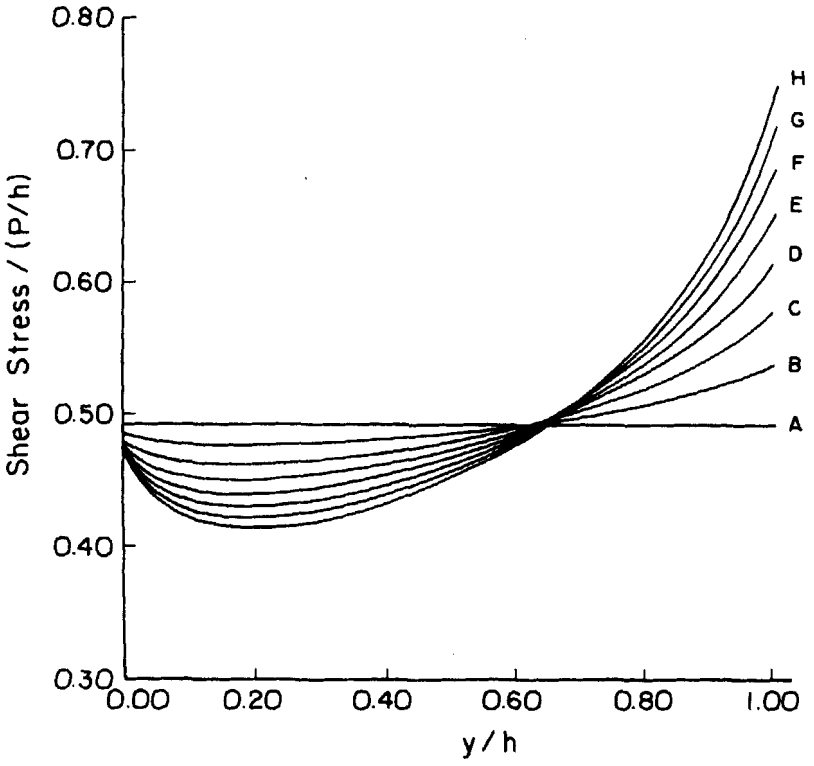

FIGURE 2 Normalized Shear Stress Distribution at $x = 0$ for the shear pullout problem.

The normalized shear stress distribution generated during the shear pullout of the insert is plotted in Figure 2 for all k_s values considered, as a function of the (non-dimensionalized) distance from the free surface. As given in Table II, the curve identified by *A* corresponds to the case where the adhesive has the least rigid shear spring constant $k_s = 2.2 \times 10^4$ lbs/in.^{3} At the other extreme, curve *H* gives the shear stress distribution for the case where the most rigid adhesive is used. This figure shows that the shear stresses attain their maximum values near the tip of the insert, and that they are smallest near the free surface of the half plane. It should be reiterated here that although singularities are put in when the adhesive is assumed rigid for the first iteration (see equation 3.2), this is merely the

first step in an iterative process. The final adhesive stress distribution will not be singular, since the presence of elastic springs tends to "relax" such behavior near singular points. In the lower limiting case, A, the variation is not detectable and the stresses are constant along the insert. The difference between the shear stresses near the tip and those near the free surface is most pronounced for the case involving the most rigid adhesive. As the rigidity of the adhesive increases these results converge to the ones obtained for the "perfectly bonded" case,[6] where the adhesive is taken as rigid. It should be noted that *only this case* will produce the singularities encountered at bimaterial interfaces. All cases replacing the adhesive with a series of linear springs will result in nonsingular bond stresses. It is also interesting to note that the curves seem to "pivot" about a point near which the value of y is approximately 65% of h. This behavior of the shear stresses is predicted by a simple 1-D model analysis, in which a finite rigid strip is elastically bonded to a semi-infinite elastic strip and loaded by an end force so that the adhesive undergoes shear deformation.†

These results show that the adhesive will tend to fail (yield) near its tip first. This will result in a redistribution of the stresses along the bond line. This type of non-linear behavior will be investigated in future work.

The non-dimensionalized normal stress distribution is shown in Figure 3 as a function of the normalized distance from the free surface. For clarity, only the two extreme cases are plotted. These figures show that the maximum normal stresses occur near the free surface, and they tend to zero as y approaches h. It is also observed that these stresses vary significantly with k_s only at their extreme values near $y = 0$. There, the stress increases with increasing k_s. Away from $y = 0$, the normal stress distributions seem to be independent of the rigidity of the adhesive.

These results are significant, especially when viewed in light of the shear stress results (Figure 2). When the adhesive fails in shear, initially near the tip, residual compressive stresses, such as those encountered in fiber reinforced composite materials,[1,15] would tend to keep the debonded surfaces in contact, thus inducing friction forces in the failed region. This in turn would tend to counter shear propagation of the crack at the fiber-matrix interface. Since the normal stresses

† This 1-D model comparison was pointed out by Professor P. J. Torvik, Air Force Institute of Technology.

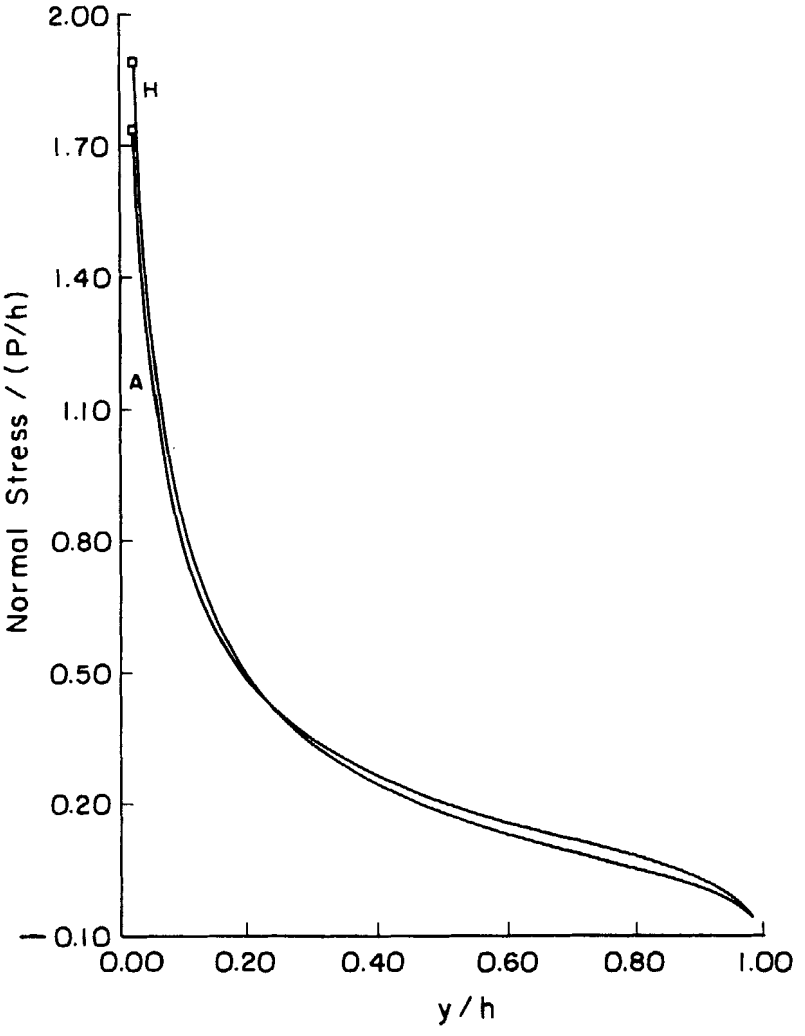

FIGURE 3 Normal Stress Distribution (non-dimensionalized) at $x = 0$ for the shear pullout problem (maximum and minimum k_s only).

in this region are negligible, the residual stresses would dominate and the crack surfaces would remain in contact. However, as the adhesive's damaged zone increases in length, thus moving away from the tip, the normal stresses increase, and at some distance from the tip they will balance the residual compressive stresses, thus eliminating friction.

Beyond that point, the growth of the damaged zone may accelerate under the combined action of the shear stresses and of the normal stresses, until complete debonding is reached. This suggested failure process seems to be in very good agreement with the experimental results obtained by Atkinson, *et al.*[16] for the axisymmetric case.

The results obtained from the solution of the problem involving the edge crack subjected to opening pressure are plotted in Figure 4. The crack opening displacements are symmetric about the $x = 0$ axis (see Fig. 1). The curves shown represent the opening at either side of the insert as a function of (normalized) distance from the free surface. Thus, these are the displacements which are multiplied by the tension spring constant, k, to obtain the resistance to opening due to the adhesive.

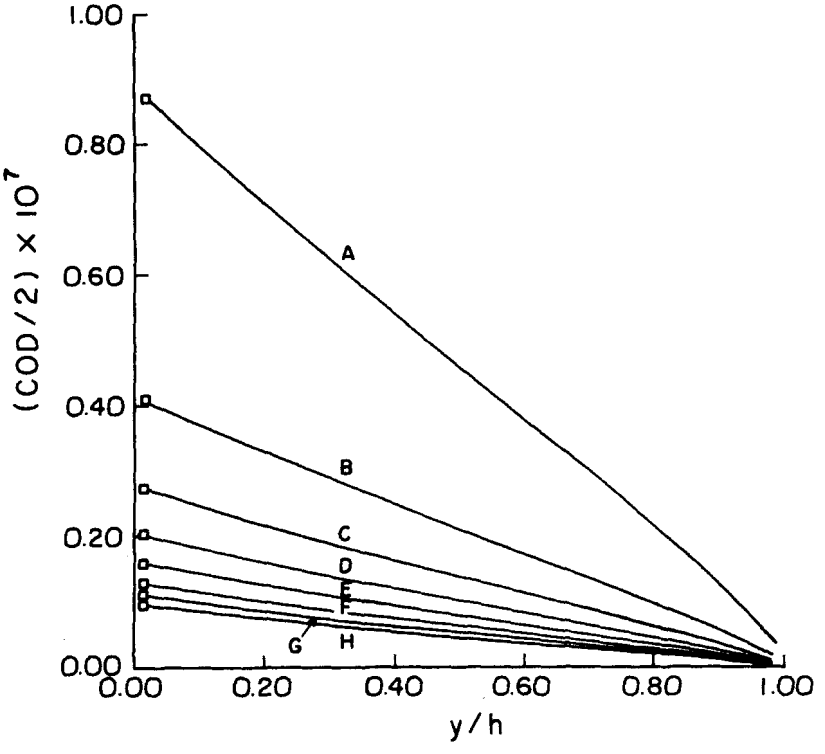

FIGURE 4 Crack Opening Displacements at $x = 0$ for the opening problem.

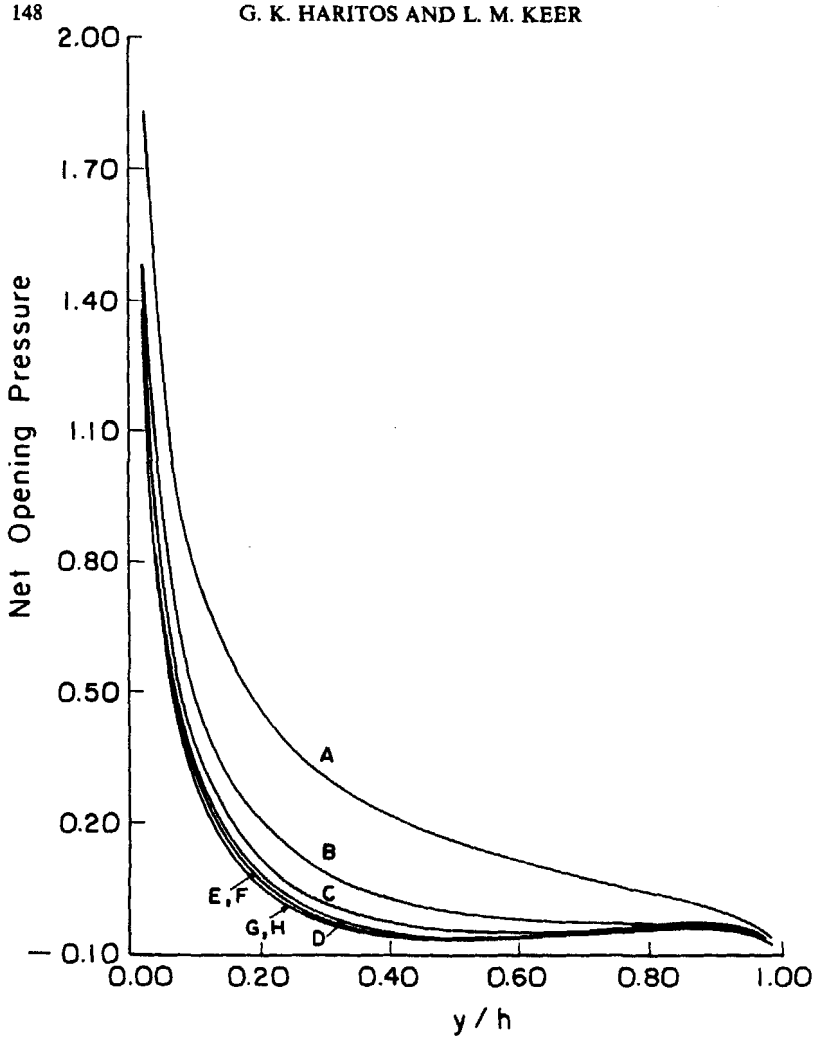

FIGURE 5 Normalized Net Opening Pressure $\frac{h}{P}\left[\tau_{xx} - k\left(\frac{COD}{2}\right)\right]$ at $x = 0$ for the opening problem.

These results show that the opening displacements increase with decreasing adhesive stiffness, k. This is what one would expect, considering the opening pressure, τ_{xx}, does not vary substantially for different adhesive materials (k_s), as shown in Figure 3, while the resistance to opening, $k(COD/2)$, increases considerably with increasing k. Thus,

the magnitude of the right-hand side of eqn (2.15) is very sensitive to the magnitude of k. This is shown in Figure 5, where the normalized "net" opening pressure, $-\frac{h}{P}\left[-\tau_{xx}+k\left(\frac{COD}{2}\right)\right]$, is plotted for all cases as a function of distance from the free surface. This figure shows good agreement between the applied "net" opening pressures (increasing with decreasing k) and the crack opening displacements shown in Figure 4.

It should also be noted that the crack opening displacements near the tip ($y = h$) are between one and two orders of magnitude smaller than the ones near the surface ($y = 0$). This behavior is consistent with the variation in the net opening stresses plotted in Figure 5. Thus, the crack is essentially closed over a portion of its length near the tip of the insert, and the length of the closed segment increases with k. It should be emphasized here that this analysis does not account for any residual compressive stresses that may be introduced during the manufacturing processes. The presence of any such stresses would clearly tend to increase the length over which the crack is closed.

Acknowledgements

The authors are grateful for support from the Frank J. Seiler Research Laboratory (U.S. Air Force). Portions of this investigation were completed while G. K. Haritos was at the Department of Engineering Mechanics, U.S. Air Force Academy. The authors are grateful to Mr H. S. Schwartz of the Air Force Wright Aeronautical Laboratories for providing them with data for adhesive materials. L. M. Keer is grateful for partial support from the National Science Foundation, Grant No. MEA 8117106.

List of symbols

A, B, C, D, E, F, G, H	Adhesive Materials Designations
A	Coefficient Matrix
$B(y)$	Dislocation Densities
c_1, c_2	Constants
COD	Crack Opening Displacements
$D(y)$	Stress Discontinuities
E	Young's Modulus

G	Shear Modulus of Adhesive Materials
h	Embedded Length of Insert
k	Equivalent Adhesive Spring Constant (Tension)
k_s	Equivalent Adhesive Spring Constant (Shear)
$K(y,t)$; $L(y,t)$	Integrand Functions
M	Coefficient Matrix
N	Half the Number of Collocation Points
P	Applied Load
t	Adhesive Thickness
u_o	Rigid Insert Displacement
u_x, u_y	Half Space Displacements
x, y	Coordinates
κ	Half Space Material Constant
μ	Half Space Shear Modulus
ν	Poisson Ratio
τ_{xx}, τ_{xy}	Normal and Shear Stresses
τ_{xx}^c	Crack Opening Pressure

References

1. T. R. Brussat and R. A. Westmann, *J. Composite Materials* **8**, 364 (1974).
2. C. C. Chamis, *Composite Materials* **6**, L. J. Broutman and R. H. Krock, eds., (Academic Press, NY 1974), p. 31.
3. D. L. Potter, Primary Adhesively Bonded Structure Technology (PABST), AFWAL-TR-80-3112 (1980).
4. A. Gerasoulis and R. P. Strivastav, *Int. J. Engng. Sci.* **19**, 1293 (1981).
5. A. Gerasoulis, *Computers and Mathematics with Applications* **8**, 15 (1982).
6. G. K. Haritos and L. M. Keer, *Int. J. Solids Structures* **16**, 19 (1980).
7. L. M. Keer and K. Chantaramungkorn, *J. Appl. Mech.* **42**, 683 (1975).
8. I. N. Sneddon, *The Use of Integral Transforms* (McGraw-Hill, NY, 1972).
9. A. Erdelyi, ed, *Tables of Integral Transforms, Vol I* (McGraw-Hill, NY, 1954).
10. V. L. Hein and F. Erdogan, *Int. J. Fracture Mech.* **7**, 317 (1971).
11. A. H. Stroud and D. Secrest, *Gaussian Quadrature Formulas* (Prentice-Hall, Englewood Cliffs, NJ, 1966).
12. A. Abramowitz and I. A. Stegun, *Handbook of Mathematical Functions* (Dover, NY, 1965).
13. E. J. Hughes and J. L. Rutherford, *Selection of Adhesives for Fuselage Bonding* Final Report No. KD-75-37 (The Singer Company, Kearfott Division, 1975).
14. *Goodyear Chemicals Advance Tech Data* (Goodyear Rubber and Tire Company, Akron, Ohio, 1979).
15. L. J. Broutman, *J. Adhesion* **2**, 147 (1970).
16. C. Atkinson, J. Avila, E. Betz and R. E. Smelser, *J. Mech. Phys. Solids* **30**, 97 (1982).